University of Leicester

The influence of IMF strength and orientation on magnetotail dynamics

エイドリアン　グロコット

Adrian Grocott

Institute of Space and Astronautical Science, Japan Aerospace Exploration Agency

2010年7月28

Outline

1. Background: IMF control of geomagnetic activity
2. Introduction to the SuperDARN radars
3. B_Y-dominated, northward IMF magnetotail dynamics
4. B_Y-dominated, southward IMF magnetotail dynamics
5. Summary

1. Background: IMF control of geomagnetic activity

Strongly northward IMF ($\theta_{IMF} < \pm 10°$) gives rise to dual lobe reconnection, closing open magnetic flux and providing a mechanism for population of the cold dense plasma sheet (e.g. Imber et al., 2006)

Southward IMF results in low-latitude reconnection and open flux production, driving the magnetosphere into an unstable state and and giving rise to the range of geomagnetic phenomena associated with magnetospheric substorms (e.g. Baker et al., 1996; Grocott et al., 2002, 2004, 2006, 2009)

Prolonged intervals of strongly southward IMF can produce magnetic storms – an enhanced ring current dipolarises the magnetotail, inhibiting substorm activity and causing an excess of open flux build up in the polar cap (e.g. Milan et al., 2009)

B_Y-dominated IMF can produce open flux at the dayside magnetopause which has a strong dusk-dawn component – this penetrates into the magnetotail and produces a range of effects on the magnetospheric and ionospheric dynamics (e.g. Nishida et al., 1995, 1998; Grocott et al., 2003, 2005, 2007, 2008, 2010)

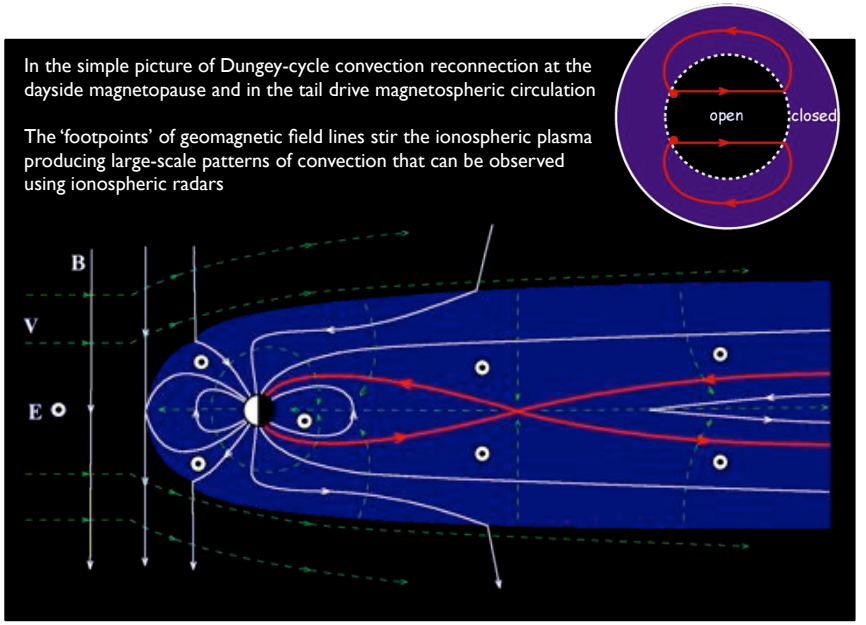

2. An introduction to the SuperDARN radars

Þykkvibær, Iceland

SuperDARN radars: Propagation Modes

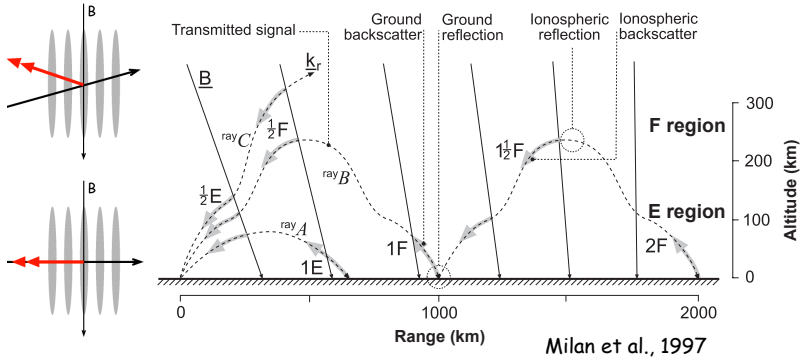

Milan et al., 1997

- Coherent (Bragg) scatter from field-aligned irregularities
- Radar wave vector must be orthogonal to the magnetic field
- HF rays refract in the ionosphere and thus achieve orthogonality at F-region heights even at high latitudes

- Backscatter can be received:
  - from both the E and F regions
  - from the ground, via oblique reflection from the ionosphere (groundscatter)
  - from far ranges, via multiple hop paths (ionosphere-ground-ionosphere)

SuperDARN radars: Measured Parameters

Spectral analysis of the backscattered signals from multipulse transmissions enable various ionospheric parameters to be calculated for a range of distances

Doppler velocity of ionospheric target

$$v_i = \frac{\omega_D}{2k_0}$$

Distance to ionospheric target

$$d = \frac{ct}{2} + v_i t$$

Doppler spectrum

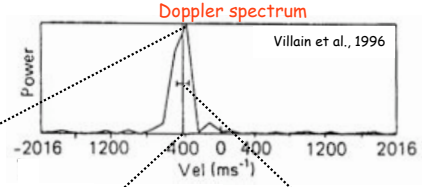

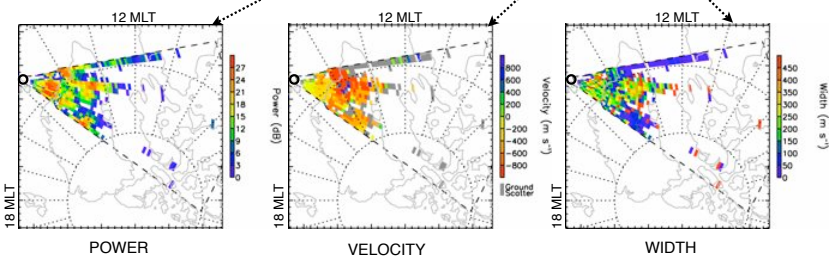

SuperDARN radars: Fields-of-View

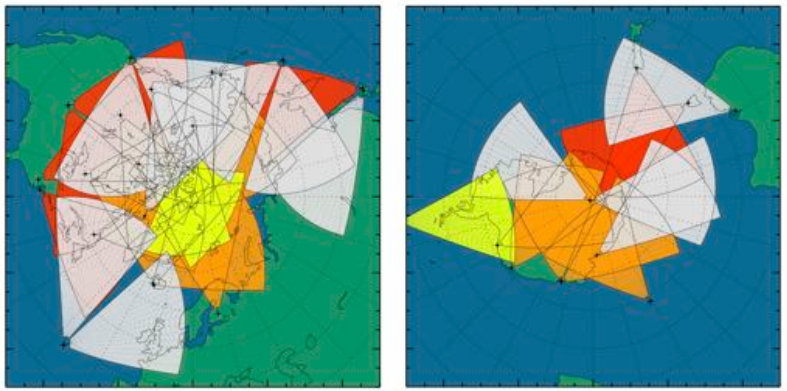

Auroral zone
Polar region

Storm time
Planned

Antarctic
Sub-auroral

Planned
Recently Operational

16 beams, 75 – 120 range gates, 15 – 45 km gate length
max. range ~ 3500 km, ~3 – 7 s beam scan time, 1 – 2 min full scan time

SuperDARN convection mapping

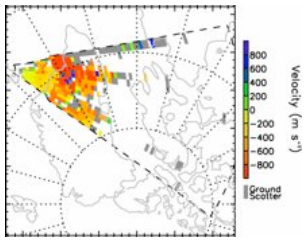

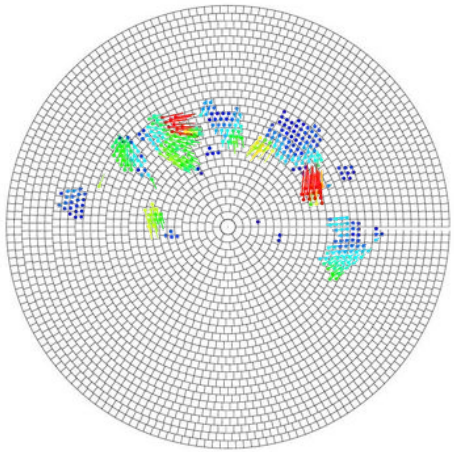

Data from each radar spatially averaged using a median filter onto an equal area grid

Average LOS velocity and standard deviation are recorded

Gridded added from other radars in the same hemisphere

SuperDARN convection mapping

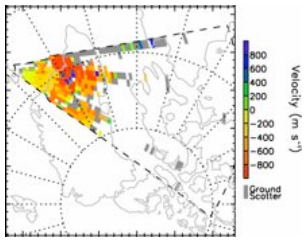

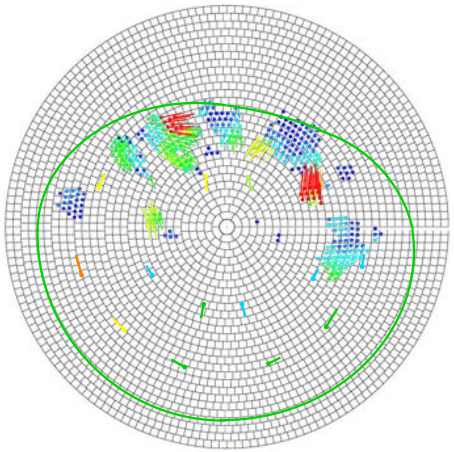

Velocity measurements from a statistical model and a zero potential boundary are added to the gridded data from all the radars, to constrain the fitting procedure

SuperDARN convection mapping

The real and model data are then fitted to a solution of the ionospheric electric potential expressed in spherical harmonics by minimising χ^2,

where:

$$\chi^2 = \sum_{i=1}^{N} \frac{1}{{\sigma_i}^2} [\mathbf{V}_i \cdot \hat{\mathbf{k}}_i - W_i]^2$$

and N is the total number of real and model data points, $\mathbf{V}_i$ is the fitted velocity vector, $\mathbf{k}_i$ is the LOS unit vector, and W_i is the line of sight velocity measurement (Ruohoniemi and Baker, 1998)

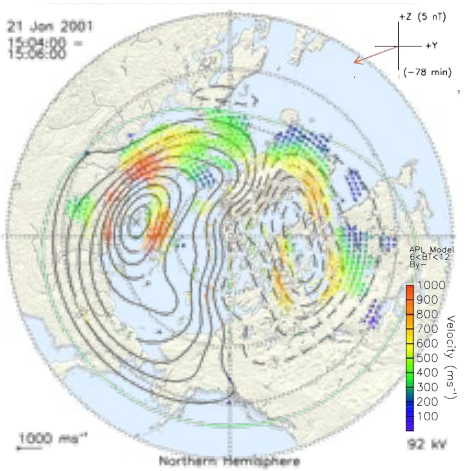

V is derived from, the potential using $\mathbf{E} = -\nabla \varphi$ and $\mathbf{V} = \frac{\mathbf{E} \times \mathbf{B}}{\mathbf{B}^2}$

3. B_Y-dominated, northward IMF magnetotail dynamics: tail reconnection during IMF northward, non-substorm intervals

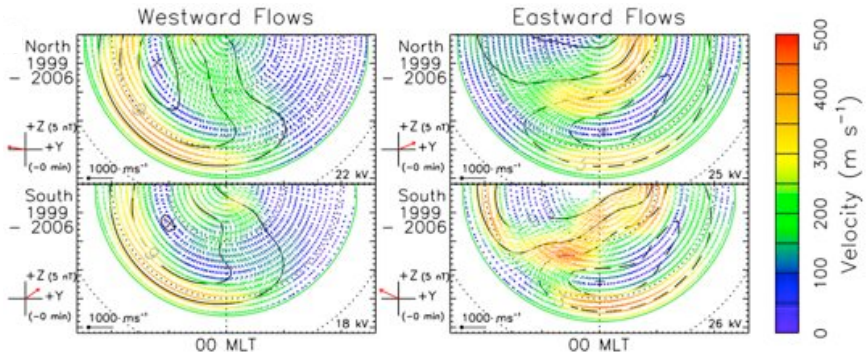

(Grocott et al., 2008)

Enhanced bursty nightside azimuthal flows

Relatively high-latitude phenomenon (>65°)

Mean AE ~100 nT

Asymmetry is opposite in opposite hemispheres

Multi-scale observations of the magnetotail

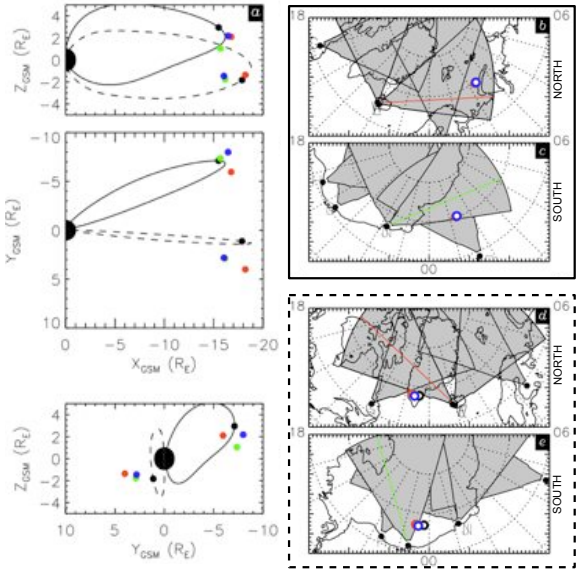

Cluster spacecraft observations of the magnetic field and ion flows in central plasma sheet in the magnetotail

SuperDARN radar observations of plasma convection in the nightside auroral ionosphere

——— B_Y < 0 interval

------ B_Y > 0 interval

Multi-scale observations of the magnetotail

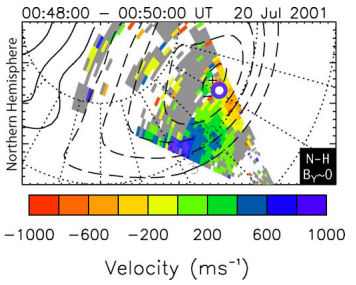

Observations from the post-midnight sector

Ionospheric radars show large-scale dawnward convection

Cluster Spacecraft reveal in-situ magnetospheric flows

Azimuthal sense of magnetospheric bursty bulk flows is consistent with post-midnight location of the spacecraft

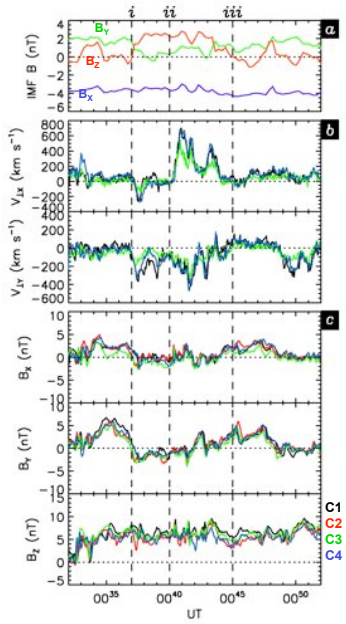

Multi-scale observations of the magnetotail

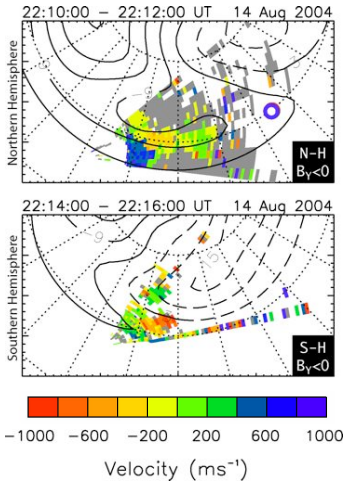

In this case, although the spacecraft is similarly located, the BBF azimuthal direction is opposite, consistent with the asymmetry in the large-scale ionospheric flows

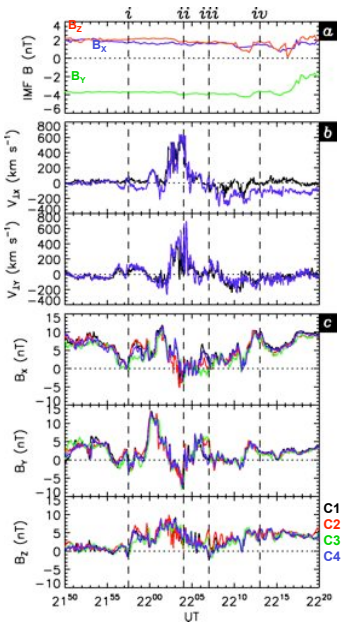

(Grocott et al., 2007)

Multi-scale observations of the magnetotail

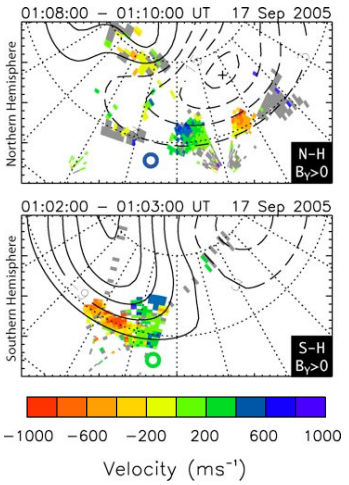

Here, the opposite asymmetry is evident in the two hemispheres, and between spacecraft on opposite sides of the tail current sheet

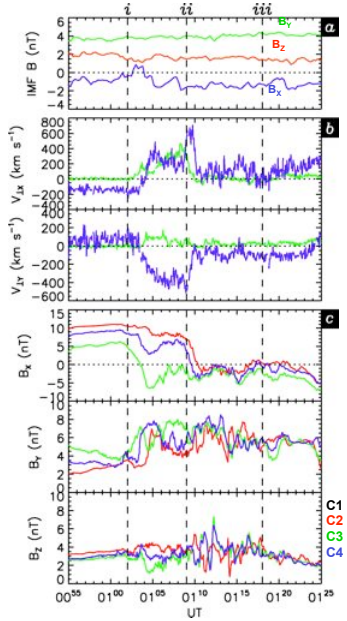

(Grocott et al., 2007)

Multi-scale observations of magnetotail dynamics

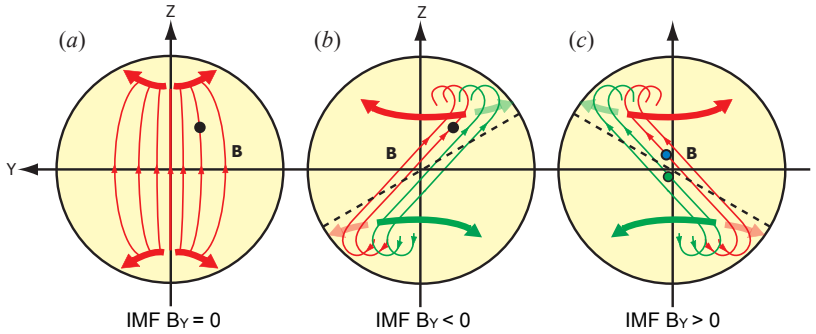

(after Nishida et al., 1998)

When IMF B_Y is zero, the azimuthal direction of the magnetotail and ionospheric flows corresponds to the MLT of the observations

When IMF B_Y is non-zero, a twist develops in the tail as IMF-reconnected field lines, added to the tail lobes, penetrate into the plasma sheet

The direction of the flows is then such that post- (pre-) midnight flows can be directed dusk- (dawn-) wards, depending on the location of reconnection in the tail, the sign of B_Y and the hemisphere of the observations

4. B_Y-dominated, southward IMF magnetotail dynamics:

a superposed epoch analysis of the ionospheric convection response to magnetospheric substorms

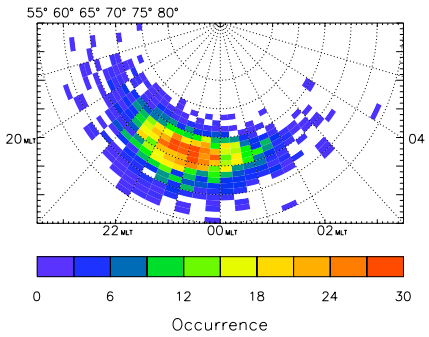

Northern hemisphere, isolated substorms identified by Frey et al. (2004)

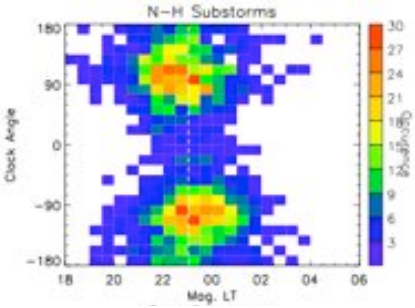

IMF clock angle versus onset MLT reveals a predominance of substorms occurring at southward, but B_Y-dominated IMF

IMF B_Y dependence of the convection evolution during substorms

We know the convection and the auroral dynamics are closely related

Onset MLT appears to be only weakly related to IMF orientation, whereas we know that the nightside ionospheric flows during northward IMF can be very strongly governed by IMF B_Y

What happens to the auroral convection when a strong IMF B_Y component exists simultaneously with the intense electrodynamics associated with substorms?

Substorm onset MLT - weak IMF B_Y dependence

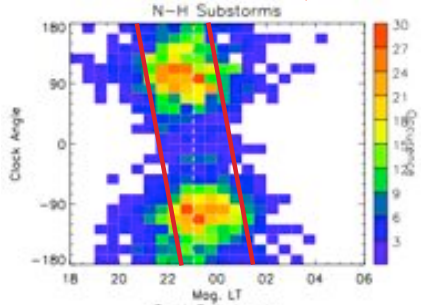

Northward IMF convection - strong B_Y dependence

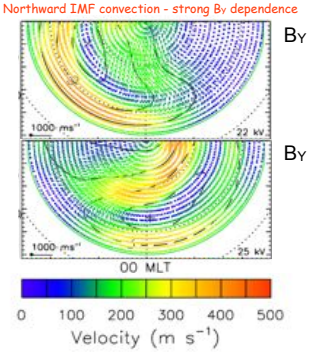

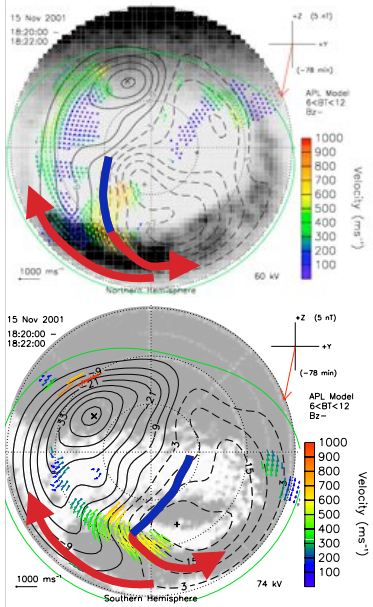

Pilot Case

15 November 2001 event

Onset is at ~ 0 MLT and expands similarly in both hemispheres

IMF B_Y has been strongly negative for > 1 h

However, the nightside auroral zone convection in both hemispheres exhibits similar asymmetries

Although insufficient dayside data exist to illustrate the B_Y-influence well, the flow reversal just poleward of the auroral oval can be seen in the southern hemisphere

Dayside and polar cap convection exhibit the expected IMF B_Y interhemispheric asymmetry

Nightside auroral zone convection shows no interhemispheric asymmetry - substorm controlled

Superposed Epoch Analysis of the IMF B_Y dependence of substorm convection

65° – 67° Lat, $|B_Y|$ > 2 nT

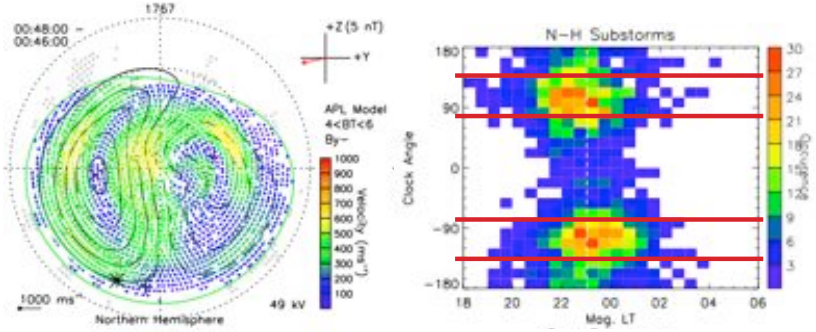

We have divided the substorms into 2 groups of opposite IMF B_Y, from a restricted latitude range, and combined the radar data to produce average substorm convection patterns from various times during a substorm

65° – 67° Lat, B_Y < -2 nT

65° – 67° Lat, B_Y > 2 nT

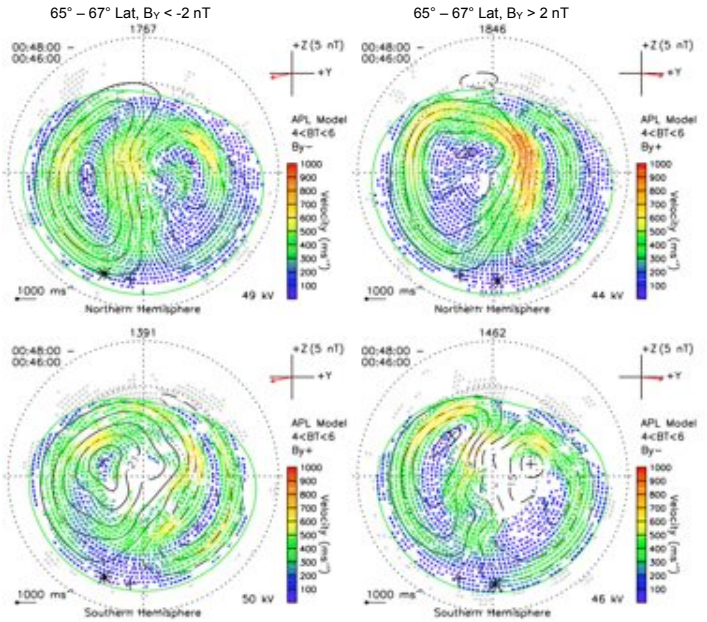

65° – 67° Lat, B_Y < -2 nT

65° – 67° Lat, B_Y > 2 nT

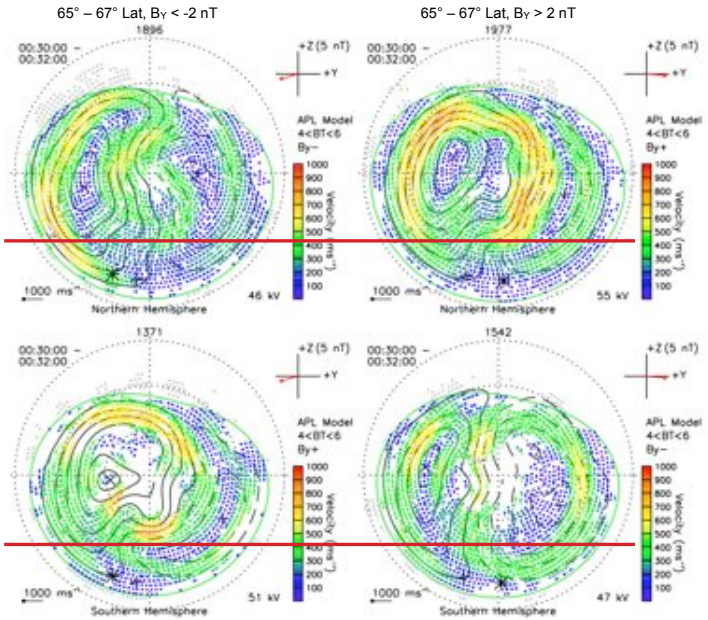

Northern (Southern) Hemisphere
B_Y -ve (+ve) non-substorm case

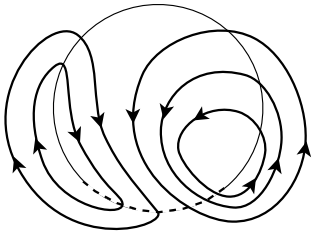

Northern (Southern) Hemisphere
B_Y +ve (-ve) non-substorm case

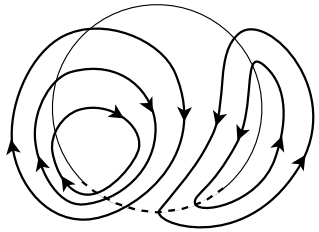

Northern (Southern) Hemisphere
B_Y -ve (+ve) substorm case

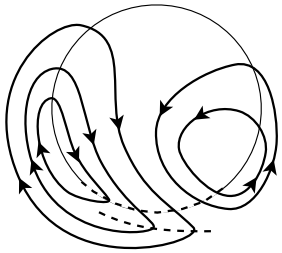

Northern (Southern) Hemisphere
B_Y +ve (-ve) substorm case

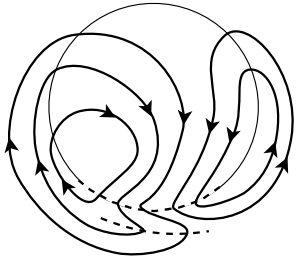

Plasma sheet morphology during substorms (Hones, 1984)

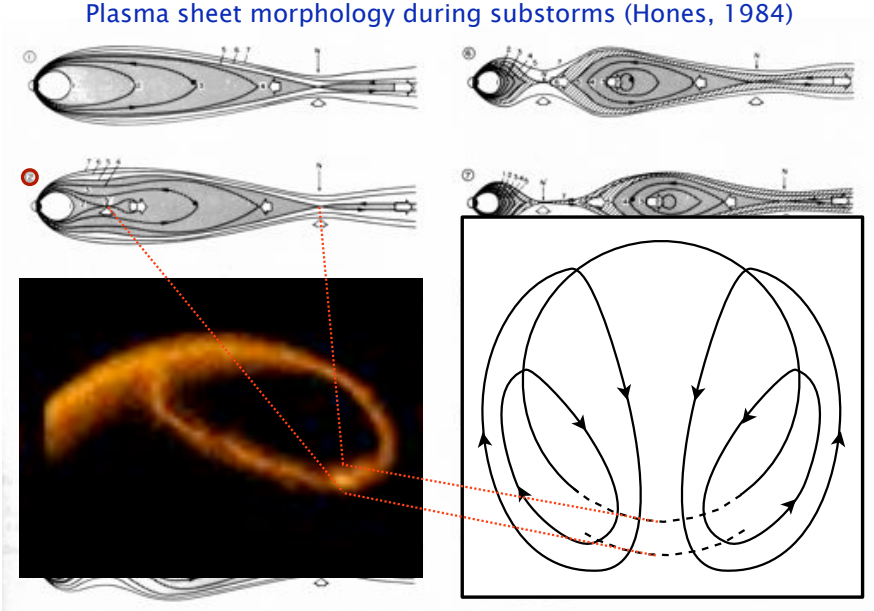

5. Summary

The ionospheric convection, as measured by the Super Dual Auroral Radar Network (SuperDARN), can provide much information about the different modes of magnetospheric activity

Whereas the dayside convection will respond near-instantaneously to changes in the upstream interplanetary conditions, different modes of activity develop as a result of the time-history of the solar wind-magnetosphere interaction

During prolonged intervals of low-level dayside loading, such as during intervals of northward IMF, the magnetosphere does not enter the substorm cycle; instead the IMF B_Y component has time to penetrate deep into the magnetotail governing the nature of the dynamics

During intervals of stronger driving, when substorm electrodynamics dominate, the IMF cannot penetrate deep into the magnetosphere, so the asymmetries associated with the IMF B_Y component give way, in the auroral zones, to intrinsic asymmetries associated with substorms